Iterative technique for analysis of periodic structures at oblique incidence in the finite-difference time-domain method

Ilya Valuev,[1,*] Alexei Deinega,[2] and Sergei Belousov[2]

[1]*Joint Institute for High Temeperatures of the Russian Academy of Sciences, 13/19 Izhorskaya Str., Moscow 125412, Russia*

[2]*Kinetic Technologies Ltd., 1 Kurchatov Square, Moscow 123182, Russia*

[*]*Corresponding author: valuev@ihed.ras.ru*

Received March 20, 2008; revised May 5, 2008; accepted May 21, 2008; posted May 29, 2008 (Doc. ID 94109); published June 26, 2008

Normal incidence of a plane electromagnetic wave on a periodical structure can be simulated by the finite-difference time-domain method using a single unit cell with periodical boundary conditions imposed on its borders. For the oblique wave incidence, the boundary conditions would contain time delays and thus are difficult to implement in the time-domain method. We propose a method of oblique incidence simulation, based on an iterative algorithm. The accuracy of this method is demonstrated by comparing it with the layer Korringa–Kohn–Rostoker frequency-domain method for calculation of transmission spectra of a monolayered photonic crystal. © 2008 Optical Society of America

OCIS codes: 000.3860, 000.4430, 290.0290.

The finite-difference time-domain (FDTD) method [1] is one of the most popular techniques employed in the computational electrodynamics. The reason for this is its relative implementation simplicity, ease of complex geometry generation, and ability to handle nonlinear media. Simulation of optical properties of periodical structures having a surface (photonic crystals, antenna arrays, etc.) is one of the applications of FDTD. Plane waves coming from a remote source are usually used to numerically obtain transmission and reflection properties of these structures. For any given point $\vec{x}$ and any field $\vec{F}(\vec{x},t)$ propagating in a planar periodic structure as a result of its interaction with a plane wave $\vec{k}$, the following condition holds:

$$\vec{F}(\vec{x},t) = \vec{F}(\vec{x}+\vec{a},t+(\vec{k}\vec{a})/(kc)), \tag{1}$$

where $\vec{a}=m_1\vec{a}_1+m_2\vec{a}_2$, $m_{1,2}\in\mathbf{Z}$ is a combination of lattice translation vectors $\vec{a}_{1,2}$, which are parallel to the structure surface. If the wave propagates normally to the surface ($\vec{k}\vec{a}=0$), the simulation may be limited to a single unit cell by imposing periodic boundary conditions: $\vec{F}(\vec{x}_b,t)=\vec{F}(\vec{x}_b+\vec{a}_b,t)$. At boundary points $\vec{x}_b$ of the unit cell the fields are mapped to the corresponding opposite boundary $\vec{x}_b+\vec{a}_b$ along periodic directions ($\vec{a}_b=\pm\vec{a}_{1,2}$ for four possible boundaries). Thus, together with the known analytic incident wave at nonperiodic boundaries the system of Maxwell equations becomes closed. If the wave is oblique to the surface, time shift

$$\Delta t_b = (\vec{k}\vec{a}_b)/(kc) = \pm a_{1,2}\sin\theta_{1,2}/c, \tag{2}$$

where $\theta_{1,2}$ are incidence angles with respect to corresponding lattice translation vectors, should also be included in the boundary conditions. It can be either positive or negative, depending on the unit-cell border location, so both retarded and advanced field values should be used at the borders. While the retarded values can be picked up from the recorded wave propagation, getting the advanced values constitutes a problem.

Several methods were proposed for solving this problem within FDTD. These methods may be subdivided into three groups. In the first group, new variables expressed via $\vec{E}$ and $\vec{H}$ fields are introduced in such a way that the time shift between the adjacent unit cells is excluded [2]. The equations for the new variables are equivalent for every unit cell but are different from the Maxwell equations and require special solution techniques, such as the multigrid approach [3] or the split-field method [4]. The stability of these methods tends to zero with increasing incidence angle, thus making simulation at large angles impossible.

Another idea is to force complex Bloch boundary conditions at the boundaries by setting in Eq. (1)

$$\vec{F}(\vec{x}_b,t) = \vec{F}(\vec{x}_b+\vec{a}_b,t+\Delta t_b) = \vec{F}(\vec{x}_b+\vec{a}_b,t)\exp(j\alpha_b),$$

thus replacing time shift with a complex phase α_b. This replacement is valid only when the incident plane wave is monochromatic with frequency ω_0 and the phase is uniquely related to the incidence angle(s): $\alpha_b=\pm\omega_0 a_{1,2}\sin\theta_{1,2}/c$. If the initial incident wave used in the simulation is indeed monochromatic, one obtains results for a single frequency and a single incidence angle per simulation, as in the sine–cosine method [5]. Alternatively, one may use a nonmonochromatic wave as a source and some selected phase α_b [6]. Then transmittance for a range of (ω, θ) pairs can be extracted from a single simulation. A drawback of these methods is transition to the frequency domain, which may hinder the advantages of the time-domain simulation.

The third group of methods stays within the standard FDTD simulation design. The simplest of these is the multiple unit cells method [7]. Additional cells

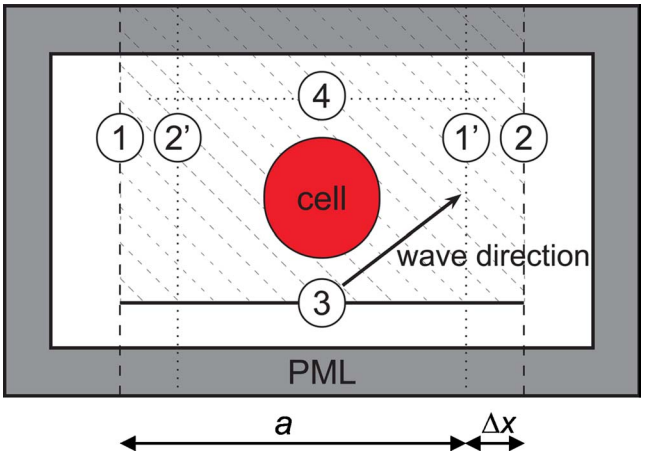

Fig. 1. (Color online) Iterative method geometry; PMLs are used to absorb scattering waves. 1, 2, generating (TF/SF) borders where transferred fields are taken as a source; 1′, 2′, corresponding image locations; 3, TF/SF border with analytic oblique source; 4, detectors for signal analysis.

are added along the direction from which the incident wave arrives; this sequence of cells is terminated by a perfectly matched layer (PML). The terminating cell is a source of error, the magnitude of which depends on the number of additional cells and the incidence angle. Additional cells are introduced in the angled-update method [1] as well, where nonsimultaneous Yee mesh updates are used. The future field values are acquired from the time-advanced adjacent cells. This method is restricted to angles less than 35° (in the 3D case).

In the following we describe our new iterative method, where the time-dependent boundary conditions are found, so that FDTD solution inside a computational volume satisfies Eq. (1). Calculation for a specific incidence angle θ needs several (5–10) simulations, which we call iterations later on. Consider a unit cell of a periodic structure of scattering objects (Fig. 1) with a surface parallel to the line 3 in the figure (the 2D case is considered for simplicity with lattice translation vectors $a_1=a$ and $a_2=0$ and time shift $\Delta t=|\Delta t_b|=a\sin\theta/c$). We use the total field/scattered field (TF/SF) technique [1] to generate a wave inside the total field region, shown shaded in Fig. 1. The time-dependent TF/SF boundary condition at border 3 represents the obliquely incident plane wave and is known analytically. Moreover, both the total and the scattered field must satisfy Eq. (1). The main idea of our method is to apply additional TF/SF-like wave generation at the side borders $\vec{x}_1$ and $\vec{x}_2$ of the unit cell using time-shifted field evolution obtained from the image points at opposite borders $\vec{x}_{1'}=\vec{x}_1+\vec{a}$ and $\vec{x}_{2'}=\vec{x}_2-\vec{a}$. For the negative time shift (data from the past), fields from the current iteration i may be used, whereas for the time-advanced fields we use the recorded evolution from the previous iteration:

$$\vec{F}_i(\vec{x}_2,t)=\vec{F}_i(\vec{x}_{2'},t-\Delta t), \tag{3}$$

$$\vec{F}_i(\vec{x}_1,t)=\vec{F}_{i-1}(\vec{x}_{1'},t+\Delta t). \tag{4}$$

The distance between borders 1 and 2 is taken greater than a by some span Δx of several mesh steps to separate image points and the TF/SF borders. To record $\vec{E}(\vec{x}_1,t)$ and $\vec{H}(\vec{x}_1,t)$, a memory buffer of $6NT/dt$ entries is required, where T is the duration of the simulation, dt is the mesh time step, and $N=N_yN_z$ is the number of mesh cells crossing border 1. A buffer of the size $6N\Delta t/dt$ is also required to use time-delayed fields at border 2. For time values $t<0$ and $t>T$ the transferred fields are assumed zero: $\vec{F}_i(\vec{x}_{1',2'},t)=0$. As the initial boundary condition for the first iteration, either the analytic incident wave or zero (no signal) is taken at the parts of borders 1 and 2 adjacent to the TF region. Surprisingly, the zero choice gives faster convergence for most geometries. The iterative process is illustrated by Fig. 2. When convergence is reached, the scattered fields both to the left of border 1 and to the right of border 2 must vanish. The total energy flux through these borders into the SF region can be used as a measure of numerical error (Fig. 3). To prove convergence of the process, we represent a source signal at borders 1 and 2 at each iteration i as a sum $\vec{F}_i=\vec{F}_0+\delta\vec{F}_i$, where $\vec{F}_0(\vec{x}_b,t)$ satisfies Eq. (1), and $\delta\vec{F}_i$ is some error signal. We note that because of the linearity of both Maxwell equations and the time-shift operations with respect to fields $\vec{F}_i(\vec{x},t)$, and the superposition principle, the evolution of error $\delta\vec{F}_i$ with i at each generating border may be considered separately from $\vec{F}_0$. Any such

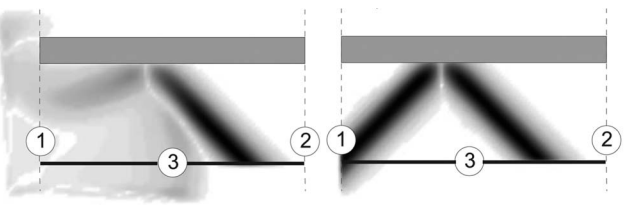

Fig. 2. First and fifth iterations of the experiment with oblique incidence on a metallic plate; $\theta=45°$ wave energy is plotted. The incident and reflected waves are clearly seen on the fifth iteration.

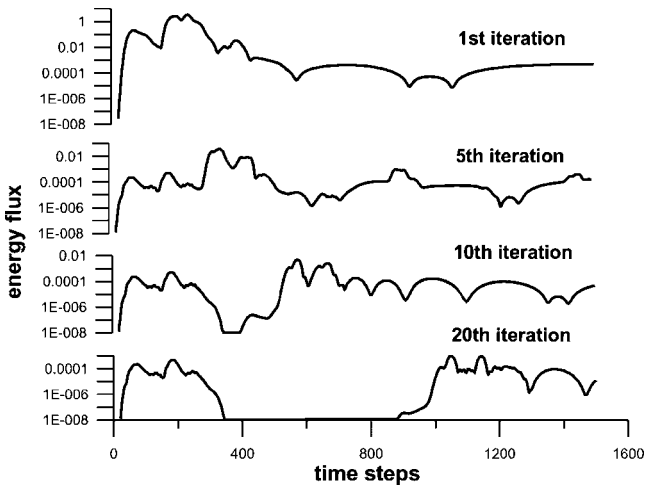

Fig. 3. Scattered field energy flux through borders 1 and 2 of the computational volume (numerical error) for the setup of Fig. 2.

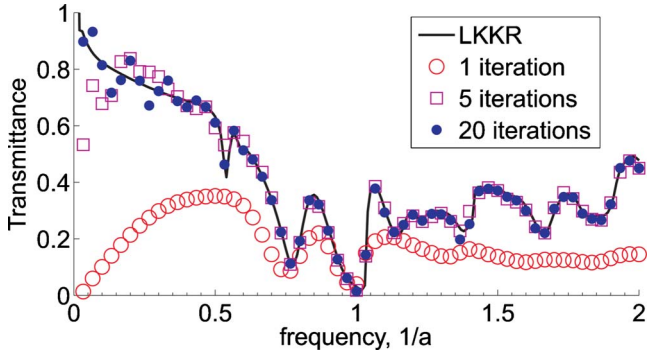

Fig. 4. (Color online) Transmittance of a photonic crystal monolayer (frequency dependence); $\theta=45°$.

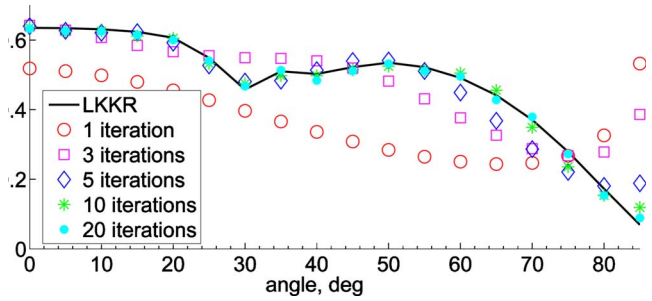

Fig. 5. (Color online) Transmittance of a photonic crystal monolayer (incidence angle dependence); $f=0.6/a$.

error will be reverted back to the source border at the next iteration with (a) positive time delay and (b) diminished amplitude. To prove these properties, observed numerically in Fig. 3, let us consider some source signal $\delta\vec{F}_i$ at border 1 with arbitrary small time duration at $t=0$. (a) The time needed for the signal to travel to the image points $1'$ is at least $\Delta t_{11'}=|\vec{x}_{1'}-\vec{x}_1|/c=a/c$. This signal is recorded at $1'$ and is transferred to 1 with advancing time shift Δt [Eq. (4)], so the total time delay is $\Delta t_1=\Delta t_{11'}-\Delta t=a(1-\sin\theta)/c$, which is greater zero if $\theta\neq 90°$. This signal is also recorded at $2'$ and reappears from 2 at the current iteration, but propagating away from $1'$ and 1. At the next iteration the error signal $\delta\vec{F}_{i+1}$ at border 1 will be zero, at least during the time interval $[0,\Delta t_1)$. The same is true for border 2 with $\Delta t_2=a(1+\sin\theta)/c$. So any source signal at borders 1 or 2 of duration T, containing some error, and not satisfying Eq. (1) will be separated from this error in time during at most $n\approx T/\Delta t_1$ iterations (the error signal is delayed by time T). In the above we assumed that the analytic border 3 may not generate error signals, which is not completely correct. Two error signals are seen in Fig. 3; the smaller, stable one accompanying the actual incident wave and related to the usual TF/SF error caused by mesh dispersion, and the "side border" error. The second error delays gradually with iterations and finally separates from the solution. (b) Because of scattering and diffraction inside the computational volume, some energy of the error signal avoids the recording image points, gets absorbed by PMLs, and is not reverted back at subsequent iterations. This reduction of error depends greatly on the properties of the scattering structure under consideration.

We implemented the iterative method as part of the generic contour-based simulation library [8]. The method has been benchmarked on a photonic crystal monolayer consisting of a square lattice of metal spheres ($\epsilon=4\epsilon_0, \sigma=2$) and subject to incident field of Berenger form $(t-t_0)\exp(-(t-t_0)^2/t_{decay}^2)$ at different angles. The lattice period was set to $a=1$, the sphere radius to 0.375, and the mesh space step to 0.05 ($c=\epsilon_0=1$). To reduce the error caused by the staircasing effect, the tensor subpixel smoothing for dielectric permittivity was used at the sphere borders [9,10]. In Figs. 4 and 5, the comparison is presented between transmittance spectra results, obtained by our method and the layer Korringa–Kohn–Rostoker method [11]. The results are in good agreement even after only five iterations, transmittance for higher frequencies and lower angles converging faster.

To conclude, we compare our method with other oblique incidence approaches. The new iterative method is free from the major drawbacks of the mentioned methods (limited/unpredictable stability, irreducible errors, large meshes, limited incidence angle, lack of direct time-domain evolution). The signal of any duration and incidence angle may be analyzed using the proposed method; however, sometimes there is a cost of large memory storage and additional iterations needed to separate error. Since the data flow per the FDTD step from the storage buffer is not very intensive, disk storage may be efficiently utilized for buffering.

This work is partially supported by the research program 15 of the Russian Academy of Science.

References

1. A. Taflove and S. H. Hagness, *Computational Electrodynamics: the Finite-Difference Time-Domain Method* (Artech House, 2000).
2. M. Veysoglu, R. Shin, and J. Kong, J. Electromagn. Waves Appl. **7**, 1595 (1993).
3. Y. C. A. Kao and R. G. Atkins, in *Proceedings of IEEE Antennas and Propagation Society International Symposium* (IEEE, 1996), pp. 1432–1436.
4. J. A. Roden, S. D. Gedney, M. P. Kesler, J. G. Maloney, and P. H. Harms, IEEE Trans. Microwave Theory Tech. **46**, 420 (1998).
5. P. Harms, R. Mittra, and W. Ko, IEEE Trans. Antennas Propag. **42**, 1317 (1994).
6. A. Aminian and Y. Rahmat-Samii, IEEE Trans. Antennas Propag. **54**, 1818 (2006).
7. J. Ren, O. P. Gandhi, L. R. Walker, J. Fraschilla, and C. R. Boerman, IEEE Microw. Guid. Wave Lett. **4**, 109 (1994).
8. I. Valuev, A. Deinega, A. Knizhnik, and B. Potapkin, Lect. Notes Comput. Sci. **4707**, 213 (2007).
9. A. Farjadpour, D. Roundy, A. Rodriguez, M. Ibanescu, P. Bermel, J. D. Joannopoulos, S. G. Johnson, and G. Burr, Opt. Lett. **31**, 2972 (2006).
10. A. Deinega and I. Valuev, Opt. Lett. **32**, 3429 (2007).
11. N. Stefanou, N. Yannopapas, and D. Modinos, Comput. Phys. Commun. **113**, 49 (1998).